Energy Injections in Gamma Ray Bursts

Y. B. Yu[1,2], X. F. Wu[3,4], Y. F. Huang[1,2,*], M. Xu[5]

[1]*Department of Astronomy, Nanjing University, Nanjing 210046, China;* [*]*hyf@nju.edu.cn*

[2]*Key Laboratory of Modern Astronomy and Astrophysics (Nanjing University), Ministry of Education, China*

[3]*Purple Mountain Observatory, Chinese Academy of Sciences, Nanjing 210008, China*

[4]*Joint Center for Particle Nuclear Physics and Cosmology of Purple Mountain Observatory-Nanjing University, Chinese Academy of Sciences, Nanjing 210008, China*

[5]*Department of Physics, Jiangxi Science and Technology Normal University, Nanchang 330013, China*

Abstract In this study, we will introduce some special events, such as GRBs 081029, 100814A and 111209A. Unexpected features, such as multiple X-ray flares and significant optical rebrightenings, are observed in their afterglow light curves, unveiling the late-time activities of the central engines. Here, we will summarize our previous numerical results of these three bursts by using the energy injection model. Especially, we will focus on GRB 100814A, with an early-time shallow decay phase and a late-time significant rebrightening in its optical afterglow light curve. To explain the complex multi-band afterglow emission of GRB 100814A, we invoke a magnetar with spin evolution as its central engine. We argue that the optical shallow decay phase and the X-ray plateau are due to energy injection from the magnetar in its early spin-down stage, while the significant optical rebrightening observed at late time naturally comes from the spin-up process of the magnetar, which is caused by subsequent fall back accretion.

Keywords: gamma-ray bursts, jets and outflows, radiation mechanism, non-thermal

1. Introduction

Gamma-ray bursts (GRBs) are bright unpredictable flashes of gamma-rays coming from deep space (for recent review, see [1]). The external shock model is usually recognized as the standard model since it can well explain the main observed features of GRB afterglows (e.g. [2], [3]), which are generally believed to be from the interaction of the relativistic outflow with the surrounding interstellar medium (ISM) (e.g. [4]). It is generally believed that long GRBs should be connected with the collapse of massive stars (e.g. [5], [6]), while short GRBs could be due to the coalescence of two compact objects (e.g. [7] – [9]).

With the advance of new observational techniques and the launch of Swift satellite, strange events, such as GRBs 081029, 100814A, and 111209A with significant optical rebrightenings or strong flares at X-ray wavelength, are observed in GRB afterglows. To explain these unexpected features, lots of different mechanisms have been proposed, such as the two-component jet model (e.g. [10]), which is somewhat different from the density jump model (e.g. [11]), the energy injection model (e.g. [12] – [18]), and the microphysics variation mechanism ([19]), which assume that the emission comes from the same emitting region. Previously, we interpreted the unexpected afterglow light curves of GRBs 081029, 100814A and 111209A based on the energy injection model, which will be summarized in this paper.

Our paper is organized as follows. The observational facts of GRBs 081029, 100814A and 111209A are presented in Section 2. The energy injection model, including the dynamical evolution of the outflow

and the radiation process, are introduced in Section 3. In Section 4, we reproduce the unusual afterglow light curves of the above three GRBs based on different energy injection forms. In the final section, we give a brief discussion and summarize our results.

2. GRB samples

The optical afterglow light curve of GRB 081029 shows many unusual behaviors. Initially, the light curve evolved in the normal way, with the simple power-law decay as predicted by the external shock model. However, at about 3000 s after the trigger, the afterglow rebrightened sharply, interrupting the smooth temporal evolution. Subsequently, at about 8000 s, a small plateau appeared in the optical afterglow light curve. Finally, after about two days, the optical afterglow light curve became flat, which may come from the contribution of the host galaxy ([20]).

Before the significant optical rebrightening of GRB 100814A from about 2×10^4 s in all seven bands detected by the Gamma-Ray burst Optical and Near-infrared Detector (GROND), there is an initial power-law decay phase with a shallow decay index of $\alpha_{\rm opt,1} = 0.57 \pm 0.02$. After the remarkable rebrightening, the optical afterglow light curve evolved into the quick decay phase. The index of the quick decay phase in seven optical bands observed by GROND is $\alpha_{\rm opt,2} = 2.25 \pm 0.08$ ([21]). Finally, the optical afterglow light curves flatten significantly after about 10^6 s, suggesting the presence of an underlying host galaxy. As for the X-ray afterglow light curve, it follows the canonical X-ray light curves proposed by Zhang et al ([22]). Initially, there is a steep decay phase, which is usually interpreted as the curvature tail of the high latitude emission ([23], [24]). From about 630 s, the X-ray afterglow evolved into a shallow decay phase with a power law decay index of $\alpha_{\rm X,1} = 0.52 \pm 0.05$, which may be the effect of a continuous energy injection ([21]). The shallow decay phase lasts until about 10^5 s, and is followed by a steeper decay phase with an index of $\alpha_{\rm X,2} = 2.1 \pm 0.1$. Interestingly to note that, due to the contribution from a nearby source, the X-ray emission remained constant after 2×10^6 s ([21]).

The X-ray afterglow of GRB 111209A was detected by the Swift/XRT 425 s after the BAT trigger ([25]). Initially, there is a shallow decay phase in the very early X-ray afterglow light curve with a best fit decay index of $\alpha = 0.544 \pm 0.003$ ([26]). During the shallow decay evolution, a significant bump appeared, making the X-ray afterglow light curve quite unusual. At the end of the shallow decay phase, the X-ray afterglow light curve entered into the steep decay phase, which is followed by a plateau with an index of 0.5 ± 0.2 and a normal decay with decay index of 1.51 ± 0.08 ([26]).

3. Energy injection model and numerical results

To describe the dynamical evolution and calculate the radiation process of beamed GRB outflows, Huang et al developed some equations ([27], [28], [29]), which are appropriate for both radiative and adiabatic blastwaves, and the calculations can be easily extended to the deep Newtonian phase ([30]). Additionally, the lateral expansion, the cooling of electrons, and the equal arrival time surface effect were all incorporated in their equations. The differential equation of the evolution of the Lorentz factor (γ) can be expressed as

$$\frac{d\gamma}{dt} = \frac{-(\gamma^2 - 1)}{M_{ej} + \epsilon m + 2(1-\epsilon)\gamma m},$$

where M_{ej} is the initial ejecta mass, ϵ is the radiative efficiency and m is the swept-up ISM mass.

In the standard external shock model, electrons will be accelerated by the shock as the blast wave sweeps up the surrounding medium. The multi-band afterglow emission arises from synchrotron

radiation of these shocked-accelerated electrons due to their interaction with magnetic field (e.g. [31], [32]). When considering the energy injection from the central engine, the differential equation of the evolution of the Lorentz factor should be modified accordingly. Previously, lots of energy injection forms have been studied by many authors. For example, Dai & Lu took the energy injection form as $dE_{inj}/dt \propto (1+t/T)^{-2}$ by invoking a new-born magnetar which is losing its rotational energy through magnetic dipole radiation as the central engine of a GRB ([12]). Zhang & Mészáros argued that the general power-law energy injection form, $dE_{inj}/dt \propto t^q$, can account for many realistic cases when q = 0 (i.e., a constant injection power) ([33]). Especially, to explain the unusual features of multi-band afterglow light curves of GRB 070610, Kong & Huang assumed the energy injection form to be $dE_{inj}/dt = Qt^q$, for $t_{start} < t < t_{end}$, where both Q and q are constants, t_{start} and t_{end} are the beginning and ending time of the energy injection respectively ([34]). Considering the above energy injection form, the differential equation for the evolution of the Lorentz factor can be modified as,

$$\frac{d\gamma}{dt} = \frac{1}{M_{ej} + \epsilon m + 2(1-\epsilon)\gamma m} \times \left(\frac{1}{c^2}\frac{dE_{inj}}{dt} - (\gamma^2 - 1)\frac{dm}{dt} \right).$$

As long as we know the energy injection form, we can calculate the evolution of the bulk Lorentz factor of the external shock, based on which, the synchrotron radiation of the shocked-accelerated electrons can be obtained.

3.1. Constant and GRB 081029

To explain the observed X-ray and optical afterglow light curves of GRB 081029, we assume the energy injection rate to be constant. In our model, we assumed two periods of energy injection, each with a constant injection rate. In order to account for the rapid optical rebrightening observed at about 3000 s, we resorted to the first energy injection, which starts at 2.8×10^3 s and lasts for about 2500 s, with a power of $7 \times 10^{47}\ erg/s$. The observed optical flat stage occurring at about 10000 s required another energy injection. The corresponding energy injection rate is $3.5 \times 10^{47}\mathrm{erg/s}$, with the starting and ending time being 8×10^3 s and 1.3×10^4 s respectively. Additionally, contribution from a host galaxy with the magnitude of $r' \sim 25$ mag is assumed to interpret the final flat stage of the optical afterglow. Figure 1 illustrates our numerical fit to the observed optical data of GRB 081029, which are taken from Nardini et al ([20]). It is shown that the observed optical afterglow light curve, especially the significant rebrightening at about 3000 s, can be satisfactorily reproduced.

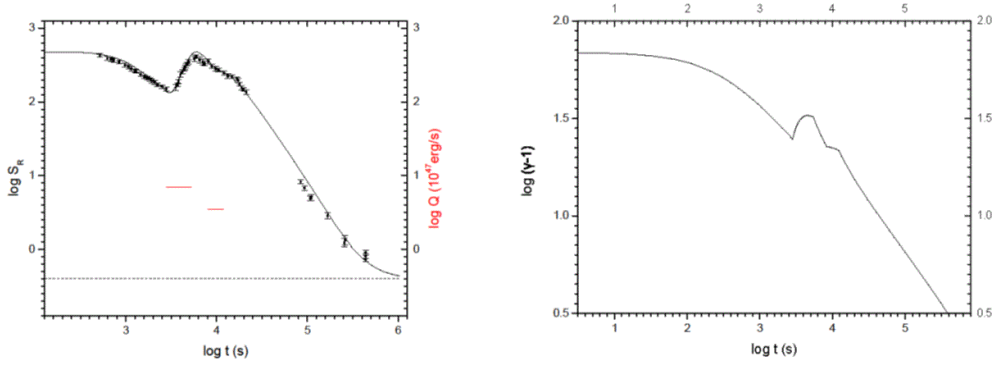

Fig1. *Left: Numerical result of the optical afterglow of GRB 081029 ([16]). The observational data were taken from Nardini et al ([20]). The dashed line is the contribution from a host galaxy with the magnitude of 25 mag. The two red straight lines represent the periods of two energy injection phases. Right: The corresponding evolution of the Lorentz factor.*

3.2. Fall back accretion and GRB 111209A

To explain the sharp X-ray rebrightening of GRB 121027A observed at about 10^3 s, Wu, Hou & Lei proposed a fall back accretion model ([35]). In this model, the central engine is assumed to be a BH. During the last stage evolution of the progenitor, part of the stellar envelope whose kinetic energy is less than the potential energy of the central BH will undergo fall back. When the fall back accretion is processing, the magnetic energy from the rotating BH can be extracted through the Blandford-Znajek (BZ) mechanism to power the GRB outflow, significantly increasing the X-ray brightness. According to Wu, Hou & Lei, the evolution of mass (M), and spin (a) of the BH are described as ([35])

$$\frac{dMc^2}{dt} = \dot{M}c^2E_{ms} - \dot{E_B}\,,$$

$$\frac{da}{dt} = \frac{(\dot{M}L_{ms} - T_B)c}{GM^2} - 2a(\dot{M}c^2E_{ms} - \dot{E_B}/(Mc^2))\,,$$

where $\dot{M}$ is fall back accretion rate. L_{ms} and E_{ms} are the angular momentum and the specific energy respectively ([36]), while T_B is the magnetic torque and $\dot{E_B}$ is the BZ jet power, which can be calculated as

$$\dot{E_B} = 1.7 \times 10^{50} a^2 (M/M_\odot) B_{15}^2 F(a)\ erg/s,$$

where F(a) is a function of spin of the central BH.

As assumed by Wu, Hou & Lei, we take the spin and mass of the BH as a = 0.9 and M = $3M_\odot$ respectively ([35]). Figure 2 illustrates our numerical fit to the observed X-ray afterglow light curve of GRB 111209A. The X-ray bump appearing at about 2000 s can be explained as due to the fall back accretion process and the peak accretion rate is assumed to be $\dot{M}_p = 2 \times 10^{-4} M_\odot/s$. To interpret the plateau observed after the X-ray bump, we invoke a constant energy injection with the energy injection rate being 9×10^{47} *erg/s*. The start and the end time of this energy injection are $t_{start} = 8 \times 10^3$ *s* and $t_{end} = 1.6 \times 10^4$ *s* respectively. The observed steep decay phase can be explained as the tail emission of the prompt phase at high-latitude, whose theoretical decay index is 2 + β_X, where β_X is the X-ray spectral index.

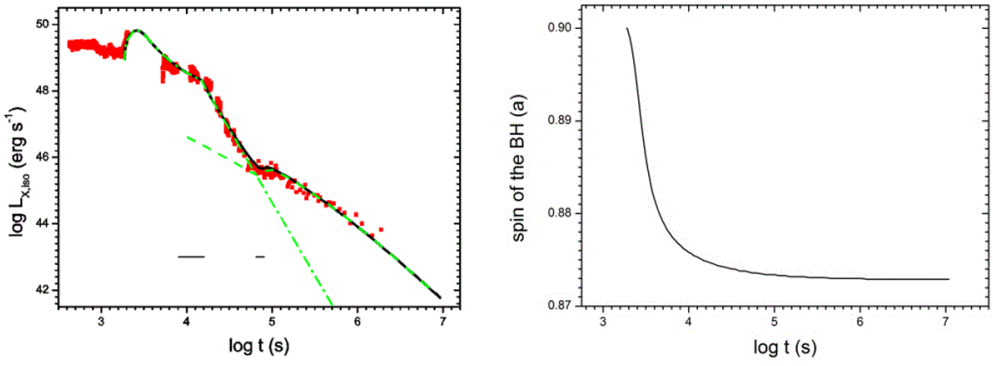

Fig2. *Left: Observed X-ray afterglow light curve of GRB 111209A and our best fit ([18]). The solid points represent the observed data from Stratta et al ([37]). The two straight lines at the bottom represent the periods of two constant energy injection phases. Right: The corresponding evolution of the spin of the central BH.*

3.3. Magnetar with spin evolution and GRB 100814A

Dai & Liu studied evolution of the GRB afterglow light curves by considering a newborn rapidly

rotating magnetar surrounded by a fall-back disk as the central engine ([38]). Initially, the magnetar is spinning down, losing its rotational energy through magnetic dipole radiation mechanism (e.g. [33], [39]). At late time, when the magnetospheric radius is smaller than the co-rotation radius, materials will fall back onto the surface of the central magnetar. As a result, the magnetar will spin up with the angular momentum of the fall back matter transferred to it and the magnetic dipole radiation luminosity will be increased, leading to a marked rebrightening in the afterglow light curve. They argued that this mechanism can naturally explain the observed shallow decay phase, plateaus, and significant brightenings in some GRB afterglows.

The spin evolution of the central magnetar can be expressed as,

$$\frac{d(I\Omega_s)}{dt} = \tau_{dip} + \tau_{acc} ,$$

Where Ω_S is the angular velocity and I is the moment of inertia. τ_{acc} and τ_{dip} are the accretion torque and the torque due to the magnetic dipole radaition respectively. During the fall back process the accretion rate initially increases with time as $\dot{M} \propto t^{1/2}$(e.g. [40]). At late time, the accretion rate evolves with time following $\dot{M} \propto t^{-5/3}$ ([41]). Therefore, the spin evolution at early and late times can be obtained as $\Omega_s \propto t^{23/28}$ and $\Omega_s \propto t^{-5/7}$ respectively, indicating that the magnetar spins up at early times and spins down at late times during the fall back process.

In our study, the central engine of GRB 100814A is assumed to be a newly born magnetar with spin evolution surrounded by a fall-back accretion disk. The early time X-ray plateau and the optical shallow decay phase can be explained well by considering the re-energized process from the central spin-down magnetar. The optical rebrightening appearing after the shallow decay phase is due to the spin-up process, which is caused by the fall-back material from the accretion disk. Compared with the significant optical bump, the amplitude of the variation observed in X-ray band is much smaller, which also can be reproduced well by our model. The observed multi-band data of GRB 100814A and our best theoretical fit are illustrated in Figures 3.

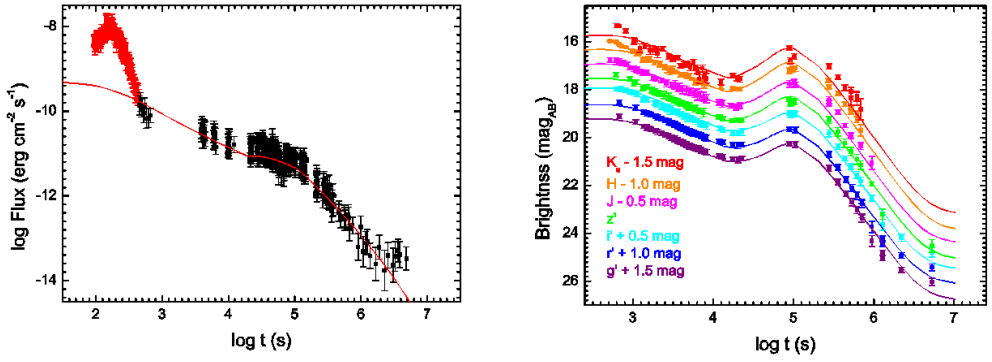

Fig3. *Left: Theoretical fit to the X-ray afterglow light curve of GRB 100814A ([17]). The points correspond to the observed XRT data ([21]). Right: Numerical fit to the seven-band optical afterglow light curves of GRB 100814A ([17]). The points represent the observational data from Nardini et al ([21]). A 0.5-magnitude shift between two adjacent light curves is applied in the plot for clarity.*

4. Conclusion and Discussion

In this study, we present a detailed study of the energy injection process and interpret the multi-band afterglow light curves of GRBs 081029, 100814A and 111209A. It is shown that the multi-band

afterglow light curves of the above three GRBs can be satisfactorily reproduced. Especially, the significant optical rebrightening of GRB 081029 observed at about 3000 s can be explained as due to a constant energy injection, the marked X-ray bump of GRB 111209A observed at about 2000 s after the BAT trigger is resulted from the fall back accretion process, while the observed optical and X-ray shallow decay phase of GRB 100814A can be interpreted by energy injection in the initial spin-down process of the central magnetar and the late time optical rebrightening can be reproduced quite well by the subsequent spin-up process.

As discussed by Yu & Huang, it is natural that there is an internal extinction in the host galaxies of cosmological GRBs due to the fact that the progenitors of long GRBs are associated with star forming regions ([16]). So when fitting the optical afterglow light curves of GRBs 081029, 100814A and 111209A, we take the extinction into consideration. There is a correction of 1.57 mag in the optical light curve of GRB 081029. The extinctions of the multi-band afterglow light curves of GRB 100814A were summarized in a table (for detail, see [17]).

To conclude, it is shown that our model is consistent with the observations of the above three GRBs. Especially, the optical rebrightening and the X-ray plateau or bump can be fitted quite well by assuming an energy injection process. It is argued that the energy injection process can be produced by materials that fall back onto the central compact object, which leads the accretion rate to increase and results in a strong outflow. In the future, more detailed studies on the energy injection and fall back processes will be helpful to provide important clues on the progenitors and the trigger mechanism of GRBs.

Acknowledgements

This work was supported by the National Basic Research Program of China (973 Program, Grant No. 2014CB845800) and the National Natural Science Foundation of China (Grant Nos. 11473012, 11322328 and 11203020). X. F. Wu acknowledges support by the One-Hundred-Talent Program, the Youth Innovation Promotion Association, and the Strategic Priority Research Program ”The Emergence of Cosmological Structures” (Grant No. XDB09000000) of Chinese Academy of Sciences.

References

[1] N. Gehrels, E. Ramirez-Ruiz & D. B. Fox, 2009, ARA&A, 47, 567

[2] M.J. Rees and P. Mészáros, ApJ Lett，1994，430：L93-L96

[3] T. Piran, 1999, Phys. Rep, 314, 575

[4] P. Mészáros and M. Rees, ApJ，1997，476：232-237

[5] S.E. Woosley, ApJ，1993，405：273-277

[6] B. Paczyński, ApJ Lett，1998，494：L45-L48

[7] D. Eichler, M. Livio, T. Piran & D. N. Schramm, 1989, Nature, 340, 126

[8] R. Narayan, B. Paczynski, & T. Piran, 1992, ApJ, 395, L83

[9] R. Perna & K. Belczynski, 2002, ApJ, 570, 252

[10] Y.F. Huang, X.F. Wu, Z.G. Dai, H.T. Ma & T. Lu, 2004, ApJ, 605, 300

[11] Z.G. Dai & T. Lu, 2002, ApJ, 565, L87

[12] Z.G. Dai & T. Lu, 1998, A&A, 333, L87

[13] M.J. Rees and P. Mészáros, 1998, ApJ, 496, L1

[14] Y.F. Huang, K.S. Cheng & T.T. Gao, 2006, ApJ, 637, 873
[15] J.J.Geng, X.F. Wu, Y.F. Huang & Y.B. Yu, 2013, ApJ, 779, 28
[16] Y.B. Yu & Y.F. Huang, 2013, RAA, 13, 662
[17] Y.B. Yu, Y.F. Huang, X.F. Wu, M. Xu & J.J. Geng, 2015, ApJ, 805, 88
[18] Y.B. Yu, X.F. Wu, Y.F. Huang, D.M. Coward, G. Stratta, B. Gendre, E.J. Howell, 2015, MNRAS, 446, 3642
[19] S.W. Kong, A.Y.L. Wong, Y.F. Huang & K.S. Cheng, 2010, MNRAS, 402, 409
[20] M. Nardini, J. Greiner, T. Kruhler et al. 2011, A&A, 531, A39
[21] M. Nardini, J. Elliott, R. Filgas, et al. 2014, A&A, 562, A29
[22] B. Zhang, Y.Z. Fan, J. Dyks, et al. 2006, ApJ, 642, 354
[23] E.E. Fenimore, C.D. Madras & S. Nayakshin, 1996, ApJ, 473, 998
[24] P. Kumar & A. Panaitescu, 2000, ApJ, 541, L9
[25] E.A. Hoversten, P.A. Evans, C. Guidorzi et al. 2011, GRB Coordinates Network, 12632, 1
[26] B. Gendre, G. Stratta, J.L. Atteia et al. 2013, ApJ, 766, 30
[27] Y.F. Huang, Z.G. Dai & T. Lu, 1998, A&A, 336, L69
[28] Y.F. Huang, Z.G. Dai & T. Lu, 1999, MNRAS, 309, 513
[29] Y.F. Huang, L.J. Gou, Z.G. Dai & T. Lu, 2000, ApJ, 543, 90
[30] Y.F. Huang & K.S. Cheng, 2003, MNRAS, 341, 263
[31] R. Sari, T. Piran & R. Narayan, 1998, ApJ, 497, L17
[32] R. Sari & T. Piran, 1999, ApJ, 517, L109
[33] B. Zhang & P. Mészáros, 2001, ApJ, 552, L35
[34] S.W. Kong & Y.F. Huang, 2010, Science China-Physics, Mechanics & Astronomy, 2010, 53(s1): 94-97
[35] X.F. Wu, S.J. Hou & W. H. Lei, 2013, ApJ, 767, L36
[36] I.D. Novikov & K.S. Thorne, 1973, Black Holes (Les Astres Occlus), 343
[37] G. Stratta, B. Gendre, J.L. Atteia et al. 2013, ApJ, 779, 66
[38] Z.G. Dai & R.Y. Liu, 2012, ApJ, 759, 58
[39] Z.G. Dai, 2004, ApJ, 606, 1000
[40] A.I. MacFadyen, S.E. Woosley & A. Heger, 2001, ApJ, 550, 410
[41] R.A. Chevalier, 1989, ApJ, 346, 847